



## Journal of Advanced Research in Fluid Mechanics and Thermal Sciences

Journal homepage:

[https://semarakilmu.com.my/journals/index.php/fluid\\_mechanics\\_thermal\\_sciences/index](https://semarakilmu.com.my/journals/index.php/fluid_mechanics_thermal_sciences/index)

ISSN: 2289-7879



# A Study on Two-Phase Flow with High Viscosity and Low Surface Tension Liquid in a 40-Degree Inclined Mini Channel

Sudarja<sup>1,\*</sup>, Sukamta<sup>1</sup>, Fitroh Anugrah Kusuma Yudha<sup>1</sup>, Muhammad Heru Susanto<sup>1</sup>, Eli Kumolosari<sup>2</sup>

<sup>1</sup> Department of Mechanical Engineering, Universitas Muhammadiyah Yogyakarta, Yogyakarta 55183, Indonesia

<sup>2</sup> Department of Mechanical Engineering, Institut Teknologi Dirgantara Adisutjipto, Jl. Janti Blok - R Lanud Adisutjipto, Yogyakarta 55198, Indonesia

### ARTICLE INFO

#### Article history:

Received 1 April 2024

Received in revised form 6 August 2024

Accepted 19 August 2024

Available online 15 September 2024

#### Keywords:

Small pipe; viscosity; flow pattern; void fraction; pressure gradient

### ABSTRACT

There are numerous applications of two-phase flow in mini pipes, including electronics cooling systems, microreactors in the chemical industry, and material development and manufacturing. This application requires a thorough understanding and is supported by complete data and information. However, the data and information are currently limited. Experimental research has been carried out on flow patterns, void fractions, and two-phase flow pressure gradients in small pipes. This study aims to obtain primary data on the subject. Dry air and a mixture of 67% distilled water, 30% glycerin, and 3% butanol represent the gas and liquid phases, respectively. The addition of butanol and glycerin each aims to reduce surface tension and improve the viscosity of the liquid phase, respectively. The density, kinematic viscosity, and surface tension of the liquid were 1,080.4 kg/m<sup>3</sup>, 2,368 mm<sup>2</sup>/s, and 38.6 mN/m, respectively. The test section was a 1.6 mm diameter glass pipe equipped with an optical correction box. The gas superficial velocity (JG) ranged from 0.025 to 66.3 m/s, whereas liquid superficial velocity (JL) varied from 0.033 to 4.935 m/s. The experiment was conducted under adiabatic conditions. Plug, slug-annular, annular, disperse bubbly, and churn flow patterns emerged, while separated flow was not discovered. For plug, slug-annular, and dispersed bubbly flows, the increase of JG proportionally affected the void fraction. However, for churn and annular flows, no particular relationship existed between JG and void fraction due to the slip between the real velocities of the gas and the liquid. The pressure gradient rose as JG and JL increased.

## 1. Introduction

Two-phase flow, which combines gas and liquid components, is commonly found in mini-channel applications across various industrial sectors. The use of two-phase flow is critical in heat exchanger systems operating in process industries, where optimizing heat and mass transfer efficiency is essential. Research by López-Belchí *et al.*, [1], Ramirez-Rivera *et al.*, [2] and Li *et al.*, [3] has documented various aspects of this phenomenon in an industrial context, including evaporators,

\* Corresponding author.

E-mail address: [sudarja@umy.ac.id](mailto:sudarja@umy.ac.id)

<https://doi.org/10.37934/arfmts.121.1.3955>

condensers, and chemical engineering equipment that rely on two-phase flow principles for thermal efficiency.

In the context of more modern cooling technologies, Kim and Mudawar [4] highlight the critical applications of two-phase flow in cooling turbine blades with water, data centers, and satellite electronic components. The importance of this technology extends to aerospace and electromobility sectors, demonstrating the urgent need for integrating two-phase flow knowledge into the development of advanced and sustainable cooling solutions. Further research by Mahvi and Garimella [5] provides a framework for predicting two-phase flow distribution in heat exchanger headers, crucial for enhancing the thermal performance of these systems. This research agrees to the investigation by Pellicone *et al.*, [6] which highlights the importance of understanding two-phase flow in the design of mini and micro heat exchangers to optimize heat exchange under highly variable flow conditions.

As summarized in Table 1, several researchers have reported their findings related to two-phase flow in mini-channels, providing insights into the different flow regimes and their impact on system performance. This compilation of research illustrates the breadth and depth of study in this field, showcasing a variety of experimental and theoretical approaches.

**Table 1**

Studies of two-phase flow pattern in mini and micro-channels in the literature

Authors	Channel configurations	Working Fluids	Flow patterns observed
Triplett <i>et al.</i> , [7]	Circular Dc = 1.1 and 1.45 mm Semi-Triangular Dh = 1.09 and 1.49 mm	Air-water	Bubbly, slug, churn, slug-annular, annular
Serizawa <i>et al.</i> , [8]	Circular Dc = 20, 25, 50, and 100 $\mu$ m	Air-water Steam-water	Bubbly, slug, liquid-ring, liquid-lump, annular
Kawaji and Chung [9]	Circular Dc = 50, 100, 250, and 530 $\mu$ m	Nitrogen-water	Bubbly, slug, churn, slug-annular, annular
Pehlivan <i>et al.</i> , [10]	Circular Dc = 800 $\mu$ m, 1 and 3 mm	Air-water	Surface tension dominated: bubbly, intermittent; Inertia dominated: churn, annular
Lee and Lee [11]	Circular Dc = 1.46, 1.8, and 2 mm	Air-water, Air-methanol	Plug, slug, annular, rivulet, stratified
Saisorn and Wongwises [12]	Circular Dc = 150 $\mu$ m	Air-water	Liquid-alone, throat-annular, serpentine-like gas core and annular
Hanafizadeh <i>et al.</i> , [13]	Circular Dc = 2, 3, and 4 mm	Air-water	Bubbly, bubbly-slug, slug, messy-slug, churn, wispy annular, ring, wavy-annular, annular
Sur and Liu [14]	Circular Dc = 0.1, 0.18 and 0.324 mm	Air-water	bubbly, slug, ring and annular
Li <i>et al.</i> , [15]	Permeable square channel 1x1 mm and 220 mm in length	Air-water	Droplet, discrete liquid film, continuous liquid film, and wavy.
Li <i>et al.</i> , [16]	Rectangular and triangle channel with Dh = 1.15 mm	Nitrogen-water	dispersed bubble, capillary bubble, slug, churn), and annular
Pipathattakul <i>et al.</i> , [17]	Circular Dc = 8, 10, and 11 mm	Air-water	Plug, slug, annular/slug, annular, bubbly/plug, bubbly/slug-plug, churn, and dispersed bubbly
Lu <i>et al.</i> , [18]	Circular Dc = 1, 2, 3 and 6 mm	Deionized water and air, nitrogen, argon and carbon dioxide	Taylor bubble interface morphologies

Authors	Channel configurations	Working Fluids	Flow patterns observed
Kim and Lee [19]	T-junction consists of a main, branch and a run with their cross section of 0.6 mm x 0.6 mm	Air-water	Bubbly, plug
Sudarja <i>et al.</i> , [20]	Circular Dc = 1.6 mm	Air-water	Bubbly, plug, churn, slug-annular, annular
Shin and Kim [21]	Rectangular Dh = 1.33 mm	Air-water	Slug, aerated-slug, transition, multiple, wavy-annular, smooth-annular, and dispersed-annular flows
Fang <i>et al.</i> , [22]	Circular parallel channel Dc = 1.5 mm	R1233zd(E)-vapor	Bubbly flow, slug flow, wavy-annular flow and local dry-out

Previous research has not explicitly combined the simultaneous effects of high viscosity and low surface tension in an inclined channel. Whereas, the application of this case is ubiquitous, such as in electronics cooling system, microreactor in chemical industry, also material development and manufacturing. Surely, the inclination of the channel varied based on the condition. Therefore, it is crucial to conduct further experimental studies that can deeply analyze the basic characteristics of multi-component two-phase flow in mini channels with an inclined orientation, aiming to explore flow patterns, flow pattern maps, void fractions, and pressure gradients in this context. The flow pattern may be recognized based on quality, flow rate, and fluid properties [23]. Understanding the complex interactions between these variables is not only important for scientific advancement but also for practical applications in engineering and system design. This research not only expands our knowledge base but also aids in the development of more efficient and sustainable technologies that can adapt to various operational conditions within the industry.

## 2. Methodology

In this study, the working fluids selected included dry air as the gas phase and a carefully formulated liquid phase consisting of distilled water, glycerin, and butanol. The choice of glycerin and butanol was strategic; glycerin was used to increase the viscosity of the liquid phase, which can influence the laminar flow characteristics and enhance heat transfer efficiency. This effect of glycerin on viscosity and its implications for flow dynamics have been elaborated upon by Ejim *et al.*, [24], who explored how variations in liquid viscosity affect droplet sizes in atomization processes, a fundamental aspect of two-phase flow systems. Butanol was employed to decrease the surface tension, facilitating improved wetting properties on the channel surfaces and promoting more stable flow patterns. Erfani *et al.*, [25] have similarly studied the impacts of alcohol mixtures, including butanol, on the surface tension in binary glycerol/alcohol mixtures, providing insights into how surface tension variations can affect interfacial behaviors.

The experimental investigation covered a wide range of superficial velocities for both phases: from as low as 0.025 m/s to as high as 66.3 m/s for the gas phase, and from 0.033 m/s to 4.935 m/s for the liquid phase [20]. Such a broad range allowed for a thorough exploration of flow regime transitions and their effects on heat transfer and pressure drops across the system. Conducted under adiabatic conditions to isolate the effects of heat transfer from external thermal influences, the experiment utilized high-speed video imaging to capture the dynamic flow patterns within the mini channels. The analysis of these images enabled accurate characterization of the void fraction, essentially the volume percentage of gas within the flow, which was further processed through advanced image analysis techniques. Simultaneously, the pressure gradient was meticulously

quantified by measuring the pressure drop across predefined sections of the channel using a highly sensitive pressure transducer. The density, kinematic viscosity, and surface tension of the liquid are  $1080.4 \text{ kg/m}^3$ ,  $2,368 \text{ mm}^2/\text{s}$ , and  $38,6 \text{ mN/m}$ , respectively.

The experimental apparatus is schematically illustrated in Figure 1. This rig, previously utilized by Sudarja *et al.*, [20], comprises several key components: an air compressor with a water trap, a pressurized tank, a working fluids mixer, a test section, a high-speed video camera, a pressure transducer, data acquisition systems, and a computer. The air compressor, which is equipped with a water trap, supplies dry air to serve as the gas phase working fluid. Additionally, the dry air acts as a liquid feeder through the pressurized tank, a technique designed to mitigate liquid pulsation, like approaches used by Kawahara *et al.*, [26] and Kawaji and Chung [9].

The test section consists of a 1.6 mm inner diameter glass pipe, 130 mm in length, outfitted with an optical correction box to eliminate distortions caused by the curved pipe surface. To capture the dynamic flow patterns within the system, a Nikon J4 high-speed video camera, capable of recording at 1200 frames per second with a resolution of  $640 \times 480$  pixels, is employed. Flow rates are meticulously measured using flow meters from Omega and TOKYO KEISO, while pressure drops along the test section are monitored using a Dwyer pressure transducer, which is integrated with an Advantech data acquisition system for enhanced precision.

As depicted in Figure 1, the liquid working fluid is pumped from a reservoir tank to a pressure tank, filled to half its capacity by a submersible pump and is subsequently pressurized by the dry air from the compressor. The liquid then continuously feeds into a perpendicular inlet mixer. Concurrently, the dry air from the compressor also flows directly into the mixer. Within the mixing chamber, the two phases, air and liquid, combine and proceed to the convergent zone, where they form distinct flow patterns before exiting into the test section. Ultimately, the mixed fluids circulate back into the reservoir tank.

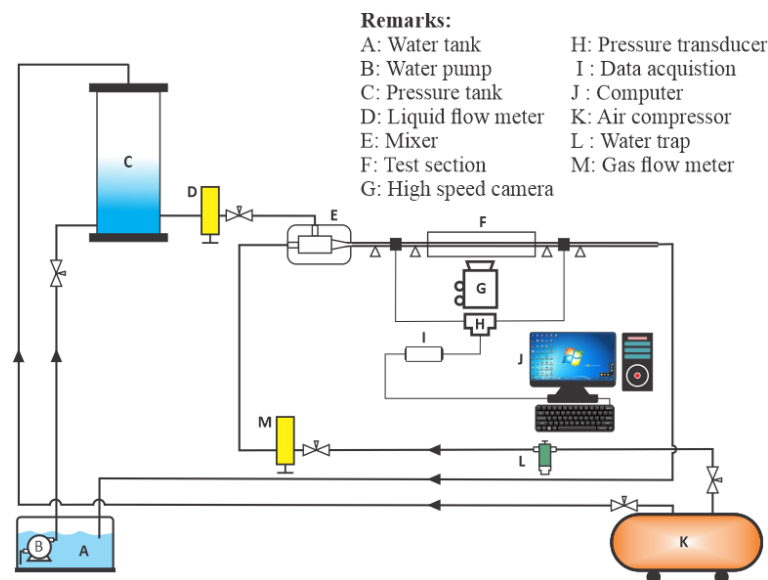


**Fig. 1.** Schematic diagram experimental rig

### 3. Results

#### 3.1 Flow Pattern Observed

In this investigation, five distinct flow patterns were identified: plug, slug-annular, annular, dispersed bubbly, and churn. Notably, the separated flow regime was absent, which may be

attributed to the predominance of surface tension forces over gravitational forces, as discussed by Chung and Kawaji [27]. Each of these flow regimes is briefly described below.

The characteristics of each flow pattern, including void fraction time series and probability distribution function (PDF), are depicted in Figure 2 to Figure 11. In these figures, part (a) displays the flow image, part (b) shows the time series of the void fraction, and part (c) illustrates the void fraction's PDF. These visual representations provide a comprehensive overview of the dynamics and statistical behavior of each flow pattern, facilitating a deeper understanding of the fluid mechanics involved in each regime.

### 3.1.1 Plug flow

Plug flow is characterized by the appearance of elongated gas bubbles intermittently separated by liquid bridges. These bubbles generally have a diameter that is the same as or slightly smaller than the inner diameter of the pipe. Typically, plug flow occurs at low to medium gas superficial velocities ( $J_G$ ) and low liquid superficial velocities ( $J_L$ ). As shown in Figure 2 and Figure 3, an increase in  $J_G$  tends to produce longer plugs and/or shorter liquid bridges. This phenomenon aligns with findings from Sudarja *et al.*, [20], which observed that lower void fraction values (less than 1, as confirmed by void fraction time series) suggest the presence of a liquid film on the outer layer of the plugs.

The influence of increased viscosity and reduced surface tension on flow patterns, particularly in plug flow, is significant. These fluid properties enhance viscous flow and wettability, affecting the stability and formation of the flow. Kovalev *et al.*, [28] explore this concept by examining the hydrodynamic features of liquid-liquid flows in serpentine microchannels, where segmented or plug flow with low viscosity ratios exhibited notable dynamics in terms of plug acceleration and deceleration influenced by channel curvature. Similarly, Tice *et al.*, [29] describe how viscosity variations affect droplet (plug) formation in microfluidic channels, further emphasizing the role of fluid properties in flow pattern development.

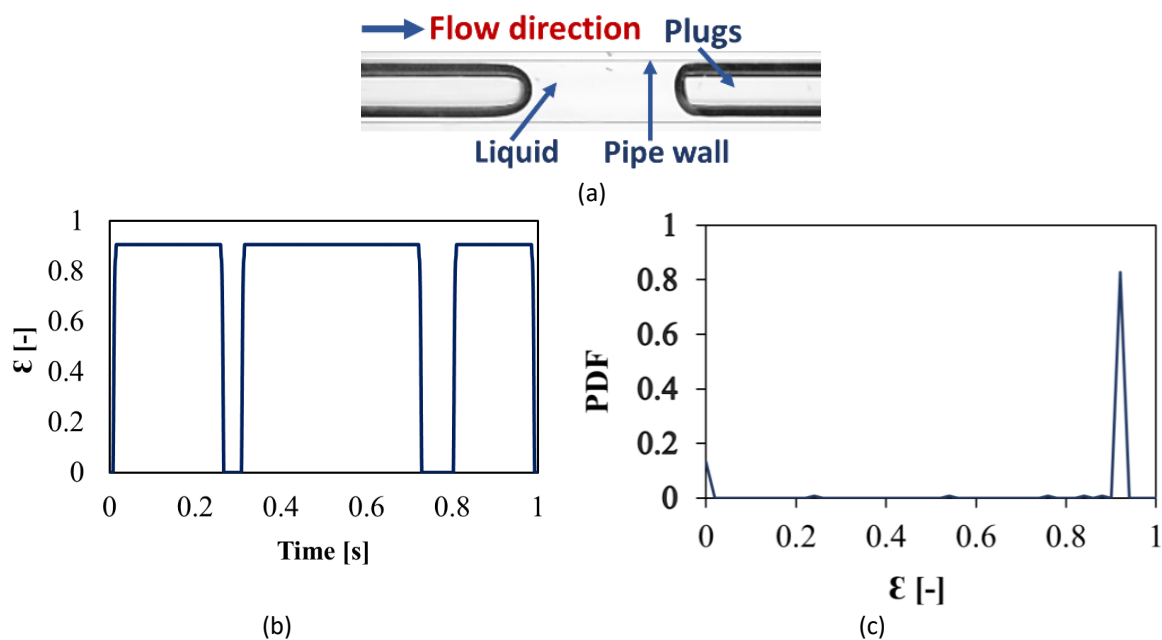


**Fig. 2.** Plug flow at  $J_G = 0.025\text{m/s}$  and  $J_L = 0.149\text{ m/s}$

The PDF used in this study, showing dominant void fraction values of 0.9 for the plug and 0 for the liquid bridge, supports the quantitative analysis of flow dynamics. This graphical representation is consistent with observations made by Kim and Lee [30], who explored how variations in surface tension impact the coalescence and breakup of gas bubbles in two-phase flows, contributing to different void fraction distributions observed in their experimental setups. Comparison of the void fraction in this study (higher viscosity) to the paper Sudarja and Sukamta [31] shows that viscosity was very influential on the void fraction. According to Sudarja and Sukamta [31], the void fraction for  $J_G$  0.066 m/s and  $J_L$  0.149 m/s is 1.0, while in this paper (lower viscosity) the void fraction for  $J_G$  0.116 m/s (higher  $J_G$ ) and  $J_L$  0.149 m/s is 0.9.

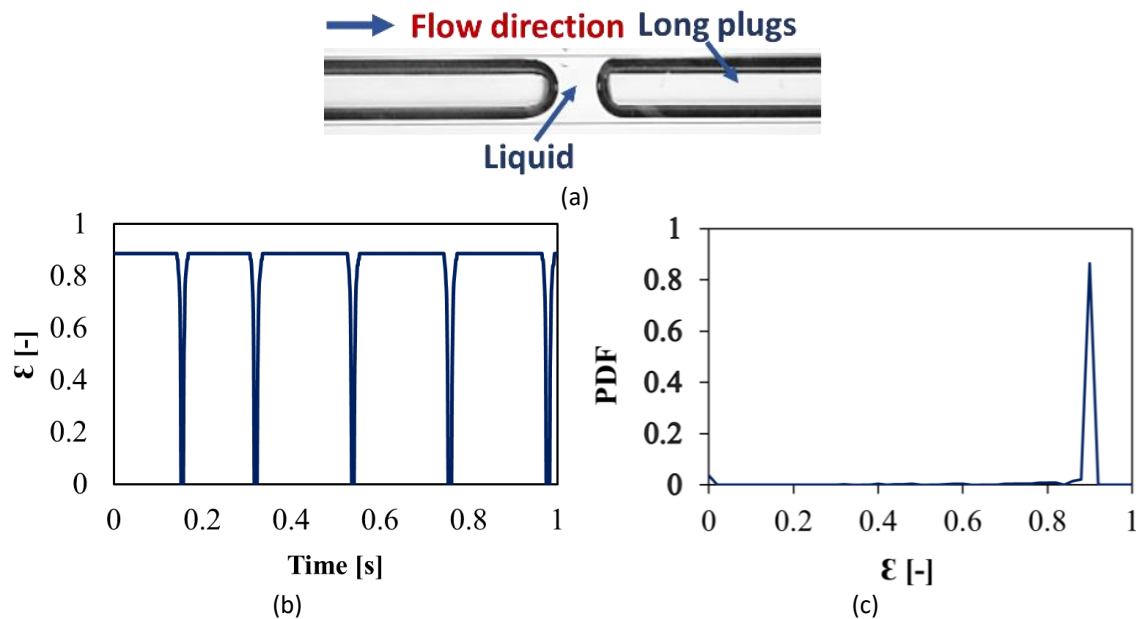


**Fig. 3.** Plug flow at  $J_G = 0.116$  m/s and  $J_L = 0.149$  m/s

### 3.1.2 Bubbly flow

In this study, bubbly flow occurred at low  $J_G$  and medium to high  $J_L$ . Notably, the bubbly flow was not a single-phase phenomenon; instances of plug flow intermittently appeared, contributing to a dispersion of the plugs' tails as observed in Figure 4 and Figure 5. These figures indicate that the most frequent void fraction recorded is zero, signifying that the flow is predominantly liquid. This observation is consistent with the effects described by Chen *et al.*, [32], who noted that increased surface tension and viscosity significantly influence slug formation and transition in microchannels, affecting the overall flow structure.

Furthermore, the morphology of the bubbles in this study differs from those observed by Triplett in 1999. Such differences likely arise from variations in fluid properties, viscosity, surface tension, and flow orientation, which play significant roles in defining bubble configuration and behavior. This agrees with findings from Boogar *et al.*, [33], who investigated the impact of viscosity and surface tension on gas-oil-water flow patterns in microchannels, demonstrating how these properties can lead to different interfacial behaviors and flow regimes.

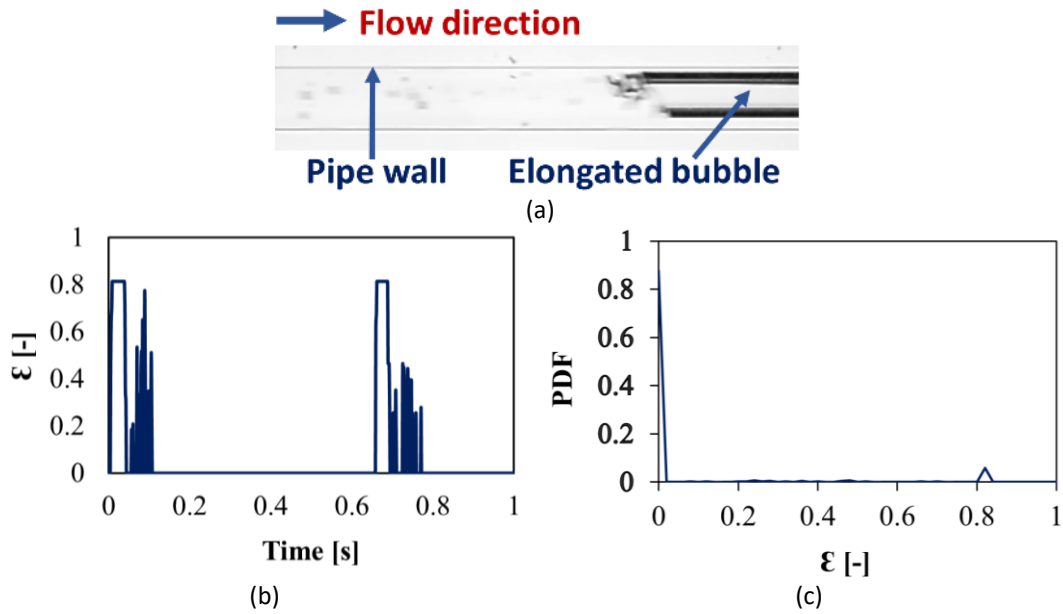


Fig. 4. Bubble flow at  $J_G = 0.025$  m/s and  $J_L = 2.308$  m/s

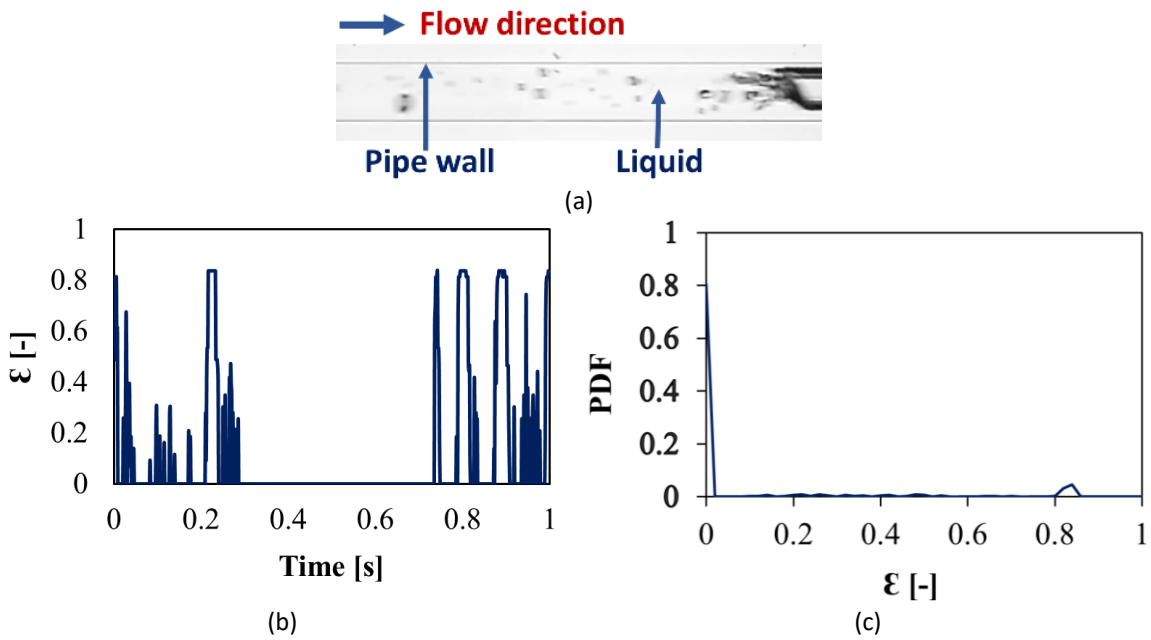


Fig. 5. Bubble flow at  $J_G = 0.116$  m/s and  $J_L = 2.308$  m/s

### 3.1.3 Slug-annular flow

In this study, as the  $J_G$  increases, gas penetrates the liquid bridges separating the gas plugs, thereby forming a liquid annulus with a gas core. Notably, the thickness of the liquid annulus varies, creating what are often referred to as liquid necks. This flow pattern is commonly identified as slug-annular flow in the literature, with various terminologies applied by different authors: Triplett *et al.*, [7] and Sudarja *et al.*, [20] use "slug-annular flow"; Saisorn and Wongwises [12] refer to it as "throat-annular flow"; Serizawa *et al.*, [8] call it "liquid ring flow"; and Sur and Liu [14] describe it as "ring flow" or "gas core with a deformed interface" by Kawahara *et al.*, [26]. This slug-annular flow pattern marks a critical transition from slug to annular flow. Characterized by periodically downward pulses in the void fraction time series, the frequency of these pulses reflects the occurrence of liquid necks.

Figure 6 and Figure 7 illustrate that an increase in JG correlates with a reduction in liquid necks, accompanied by the appearance of small-sized frothy bubbles around these necks.

The transition from annular to plug/slug flow, as examined by Kim and Lee [30], reveals that such transitions in microchannels depend crucially on mass flux and cooling rates, which influence the stability of condensate films on the walls and subsequently the formation of specific flow patterns. Additionally, Sudarja and Sukamta [31] provide further understanding of how slug scaling and liquid properties affect flow regimes in square microchannels, emphasizing the complexities of slug-annular transitions under varying conditions. This enhanced discussion not only clarifies the dynamic interplay between fluid dynamics and channel geometry but also underscores the importance of meticulous study to optimize microchannel designs for improved fluid management and heat transfer efficiency.

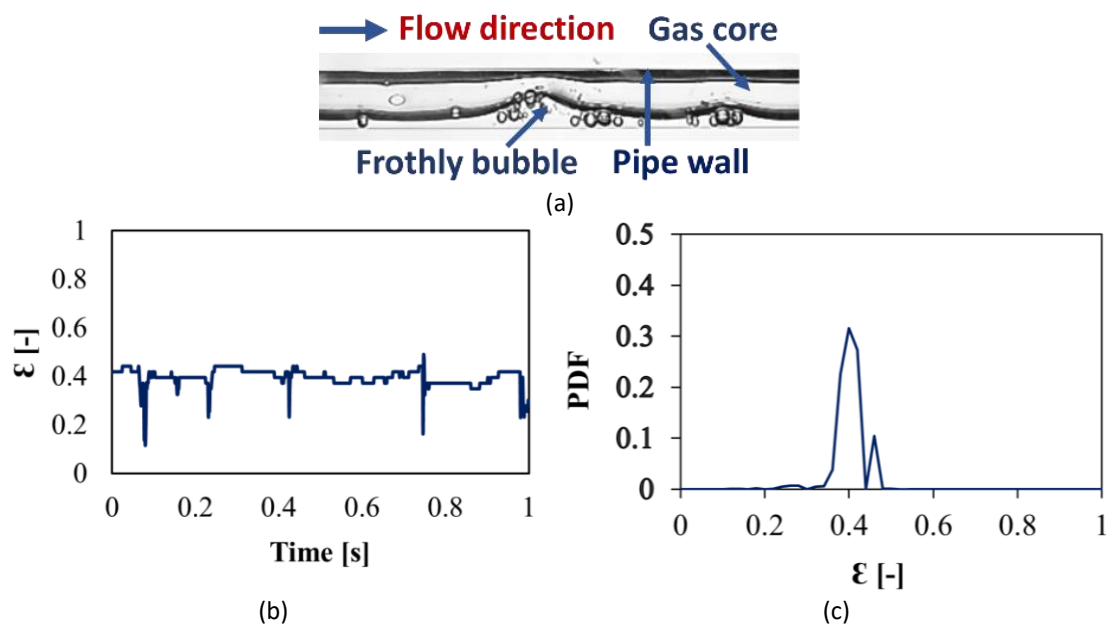


Fig. 6. Slug-Annular flow at  $J_G = 1.950$  m/s and  $J_L = 0.033$  m/s

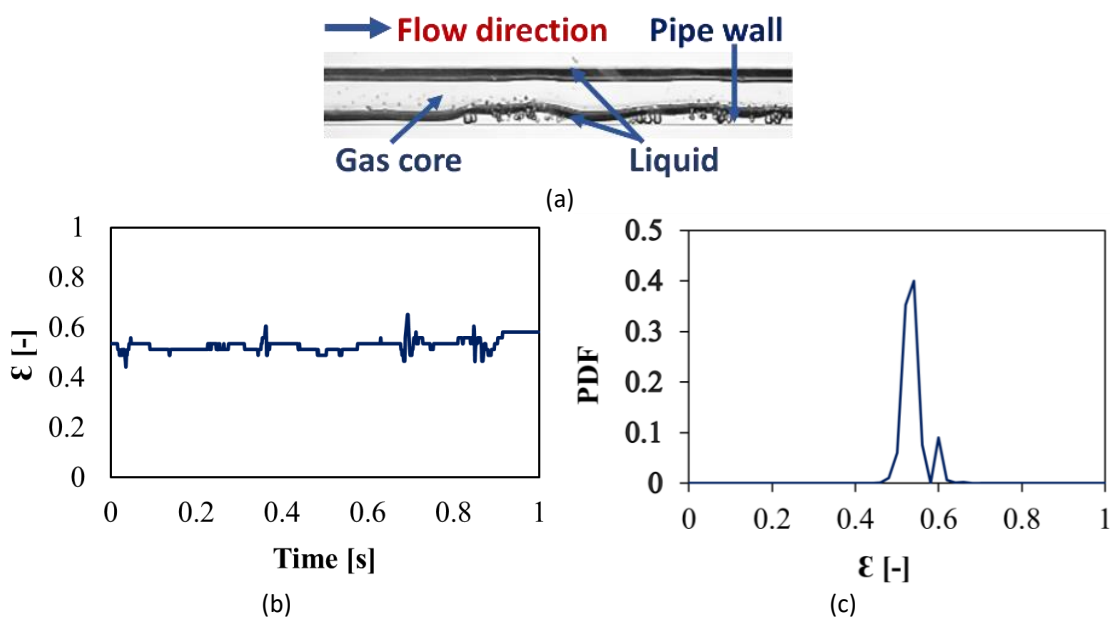


Fig. 7. Slug-Annular flow at  $J_G = 9.666$  m/s and  $J_L = 0.033$  m/s

### 3.1.4 Annular flow

As the  $J_G$  in slug-annular flow increases, the transition to annular flow is observed. This flow regime is marked by a gas core moving centrally, surrounded by a wavy liquid film adhering to the channel walls, vividly depicted in Figure 8 and Figure 9. The liquid film's wavy appearance is influenced by shear stress at the interface caused by differences in phase velocities. The wave characteristics and stability of the annular flow are significantly impacted by the fluid dynamics, particularly the viscosity and surface tension.

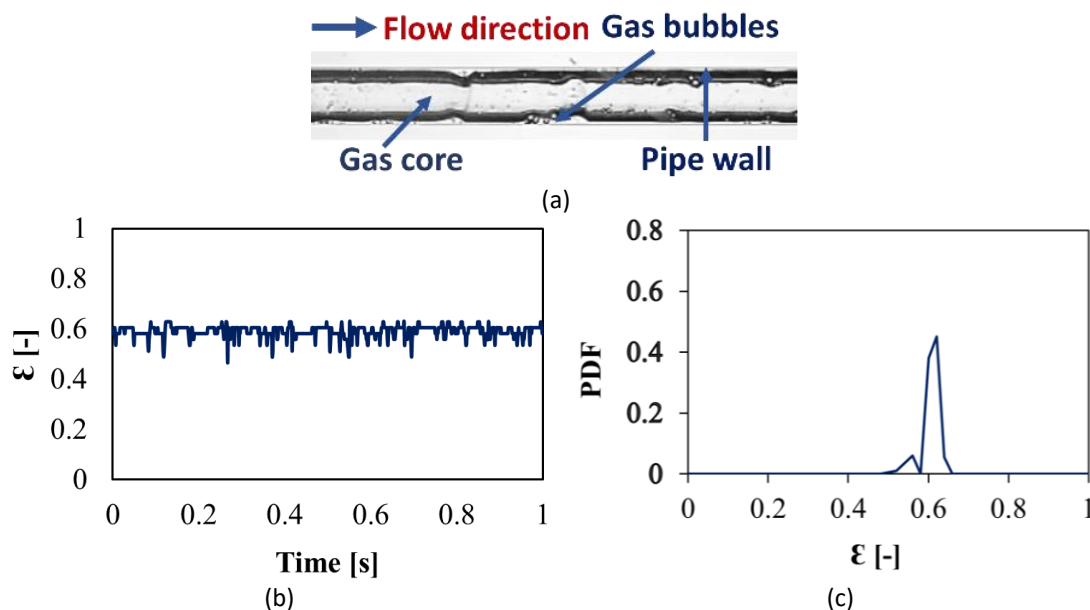


Fig. 8. Annular flow at  $J_G = 22.708$  m/s and  $J_L = 0.033$  m/s

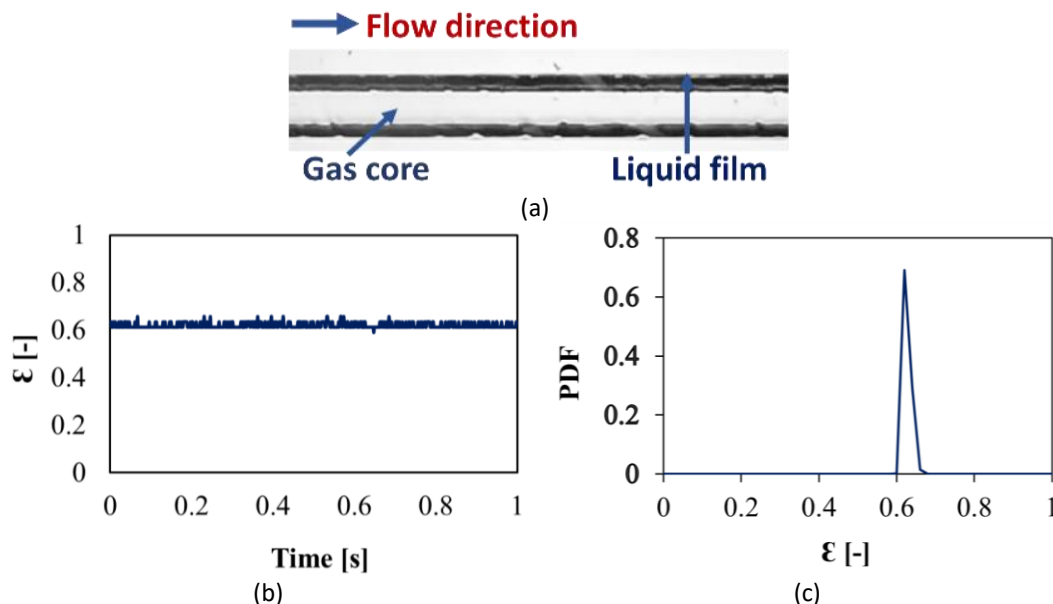


Fig. 9. Annular flow at  $J_G = 66.61$  m/s and  $J_L = 0.033$  m/s

A study by Guo *et al.*, [34] on the hydrodynamics of annular flow in microchannels through computational fluid dynamics offers insights into the behavior under these conditions. They highlighted that the flow regime is hydrodynamically unstable due to the phase interfaces being

subject to instabilities triggered by flow perturbations. This instability is echoed in the ripple curve seen in the void fraction time series, characterized by low amplitude and high frequency, indicating the prevalence of a stable, continuous liquid film.

### 3.1.5 Churn flow

Churn flow is characterized by disruptions and an irregular form due to high turbulence within both working fluids. This dynamic is vividly captured through rapid and extreme fluctuations in the void fraction time series, as illustrated in Figure 10 and Figure 11. Typically, churn flow manifests at high values of both  $J_G$  and  $J_L$ , a phenomenon also reported in studies of small pipes by researchers such as Triplett *et al.*, [7], Pehlivan *et al.*, [10], and Chen *et al.*, [32], along with more recent observations by Sudarja *et al.*, [20] and Sudarja *et al.*, [35]. These studies confirm the recurring presence of churn flow under similar conditions across various experimental setups and fluid dynamic contexts.

The studies by Yue *et al.*, [36] provide further insight into this behavior, noting that churn flow in microchannel contactors can significantly affect the two-phase flow pattern transitions and pressure drop characteristics, especially during CO<sub>2</sub> absorption processes in water. Their research highlights how flow pattern transitions, including churn flow, are not adequately predicted by existing correlations as the channel diameter decreases, leading to the development of a new empirical correlation based on the superficial Weber numbers.

In Figure 10 and Figure 11, the impact of increasing  $J_G$  or  $J_L$  on the area of the disruptive zone is demonstrated, showing that higher velocities exacerbate the turbulence and instability within the flow. This observation aligns with the effects discussed by Vozhakov and Ronshin [37], who explored how superficial velocities influence two-phase frictional multipliers in microchannels, reinforcing the complexity of churn flow dynamics.

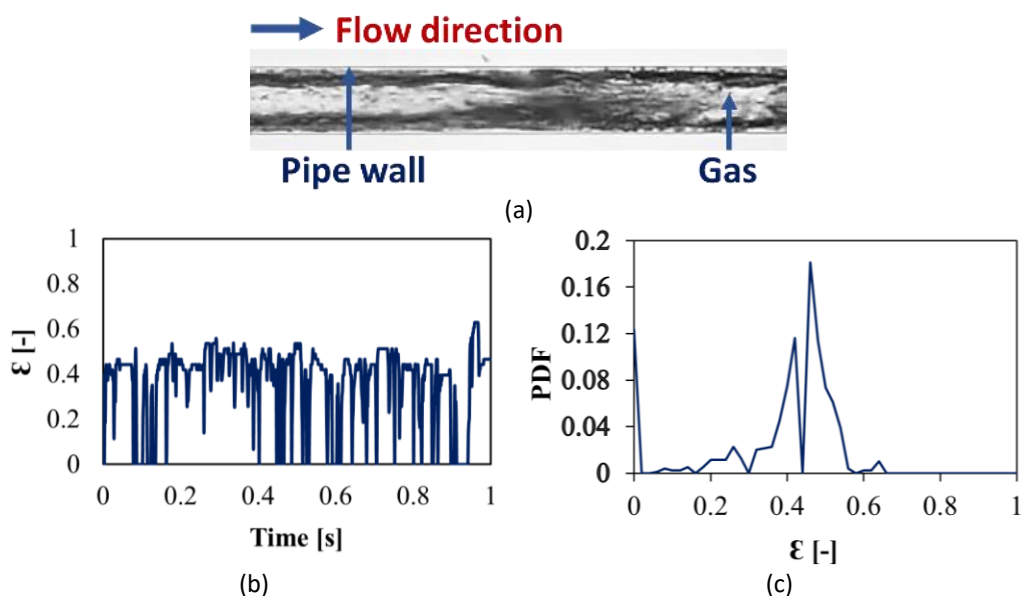
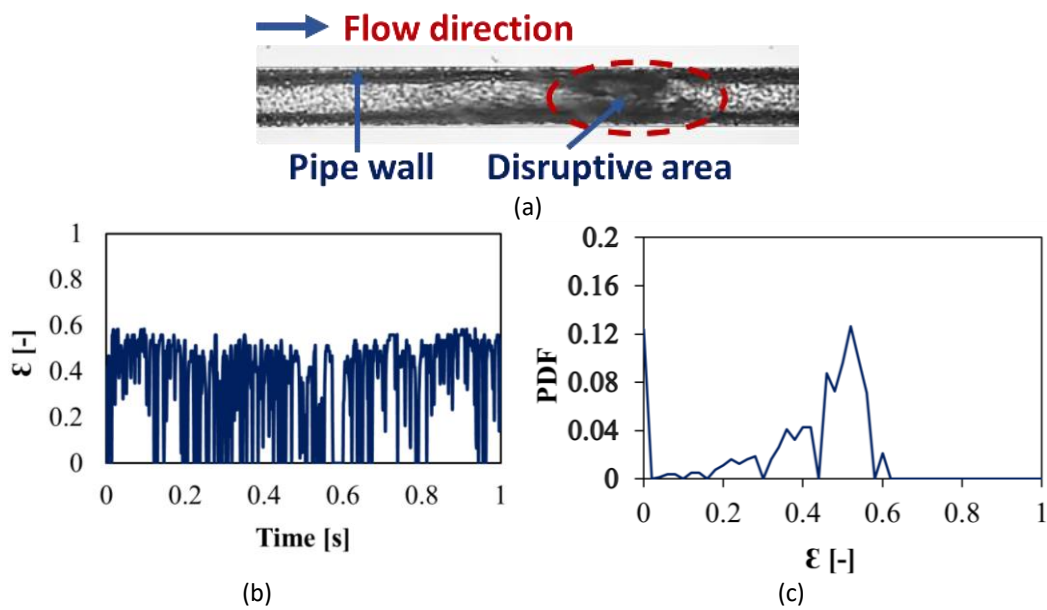


Fig. 10. Churn flow at  $J_G = 7.033$  m/s and  $J_L = 0.883$  m/s



**Fig. 11.** Churn flow at  $J_G = 9.666$  m/s and  $J_L = 0.883$  m/s

From the flow patterns mentioned above, there are some differences with the flow patterns observed in the horizontal channel. Sudarja *et al.*, [35] observed bubbly, plug, slug-annular, annular, and churn flows inside the horizontal channel with inner diameter of 1.6 mm on their experimental study. Due to the gravitational force, dispersed bubbly occurred after the breaking up of the bubble in inclined pipe. Consequently, the bubble flow did not exist.

### 3.2 Flow Pattern Map

All flow regime data from this study are systematically organized into a flow pattern map, as illustrated in Figure 12. This map features an abscissa and ordinate that respectively represent the gas and liquid superficial velocities, both scales are logarithmic to accommodate the wide range of velocities observed. Specifically, the gas superficial velocities range from 0.025 to 66.3 m/s, and the liquid superficial velocities span from 0.033 to 4.935 m/s. The author classified liquid superficial velocities depends on the flow pattern observed. At low  $J_L$ , plug, slug-annular, and annular were observed, while at medium  $J_L$ , the flow pattern obtained was plug, slug-annular, annular, and churn. The last one, at high  $J_L$ , churn and bubbly was observed.

The flow pattern map clearly shows that plug and churn flows are the most prevalent patterns under the conditions tested. This visualization allows for a quick assessment of dominant flow regimes across varying velocities, providing insights into the dynamic behavior of two-phase flow in the system.

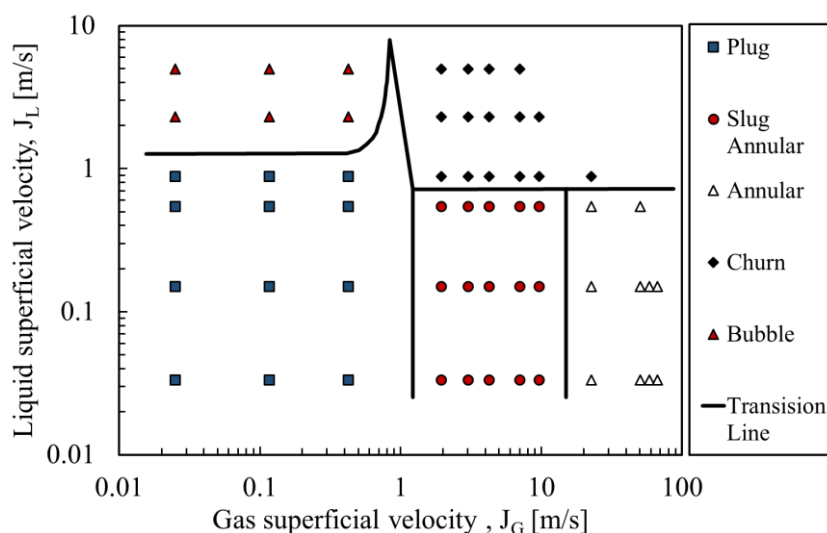


**Fig. 12.** Flow pattern map of present study

This map is then compared to previous studies, such as those by Sudarja *et al.*, [20] and Triplett *et al.*, [38], as shown in Figure 13. While there is general agreement in terms of the observed flow patterns and the configuration of boundary transition lines, discrepancies in the positions of these transition lines are evident. A notable shift is observed in the boundary transition line between slug-annular and annular flows versus churn flow. Triplett *et al.*, [38] used a 1.45 mm inner diameter pipe and deionized water, whereas Sudarja *et al.*, [20] utilized a 1.6 mm inner diameter pipe with a solution of distilled water and 3% butanol, which has a surface tension of 42.9 milli N/m. Figure 13 demonstrates that in the current study, the transition line between slug-annular to churn flow is positioned higher than in Sudarja *et al.*, [20] and Triplett *et al.*, [38], indicating that the area for churn flow is narrower in the present research, or that a larger  $J_L$  is required to initiate churn flow.

The current study, the liquid viscosity is the high, and the surface tension is the low, and the diameter of pipe is small. These conditions complicate the formation of turbulence, as the Reynolds number decreases with higher viscosity and/or smaller diameter. This phenomenon is aligned with findings by Zhang *et al.*, [39], who noted that the transition from slug to churn flow is highly sensitive to changes in liquid physical properties such as viscosity and surface tension, especially in microchannels where surface effects become more pronounced. Moreover, their research suggests that conventional models often fail to accurately predict these transitions, underscoring the need for new models or empirical adjustments based on specific experimental conditions. Many factors affect the porosity and flow transition in this paper, but there are some factors with highest impact, namely fluid properties (liquid viscosity and surface tension), superficial velocity of liquid and gas, channel  $L/d$ , and channel inclination.

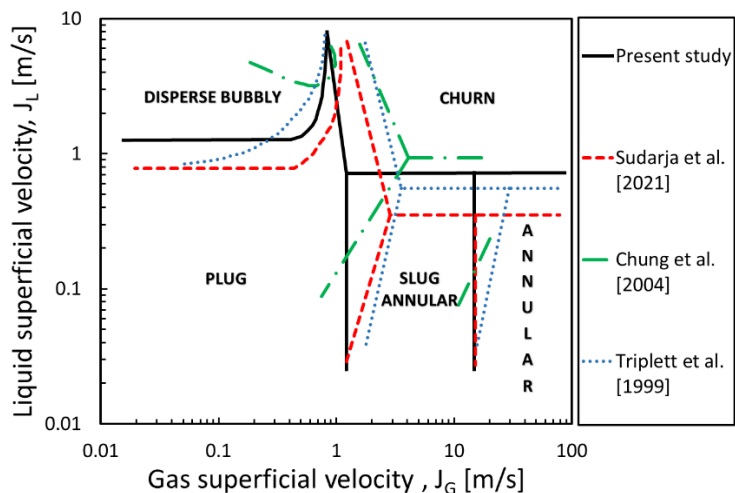


**Fig. 13.** Flow pattern map comparison present against the previous studies

### 3.3 Void fraction and Pressure Gradient

The void fraction magnitude of each pair of  $J_G$  and  $J_L$  is depicted in Figure 14. Typically, an increase in  $J_G$  corresponds to a higher void fraction. However, an anomaly is observed when the transition from plug flows to slug-annular flows occurs, where the void fraction significantly drops. This drop is attributed to the differential velocity between the gas and liquid phases, which affects the flow structure and stability. Recent studies further illuminate this phenomenon. For instance, Triplett *et al.*, [38] have observed that as  $J_G$  increases in microchannels, the interface between the gas and liquid phases becomes more dynamic, leading to variations in void fraction measurements that do not always align with simple predictive models. Their work suggests that the interactions at this interface are critical to understanding the void fraction dynamics.

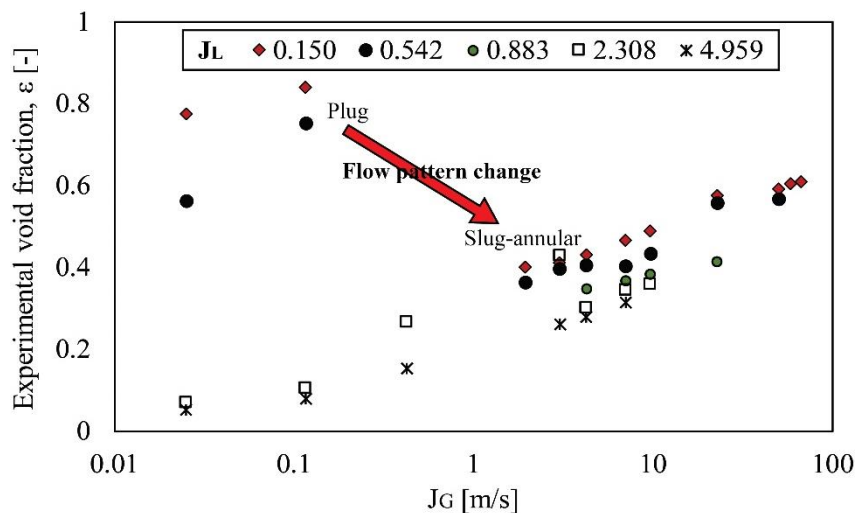


**Fig. 14.** Void fraction of each pair of  $J_G$  and  $J_L$

Furthermore, the void fraction data in this study are presented by comparing homogeneous void fractions against measured ones, as demonstrated in Figure 15. This comparison includes reference to previous studies by Kawahara *et al.*, [26]. The data reveal that for bubbly and plug flow regimes, the measured void fractions are consistently higher than the homogeneous predictions. This discrepancy suggests that the actual gas velocity within these flow regimes is lower than the actual

liquid velocity, indicating a relative retardation of the gas phase due to interactions with the liquid phase.

Conversely, for slug-annular, annular, and churn flows, the measured void fractions are significantly lower than the homogeneous estimates, implying that the gas velocity exceeds that of the liquid. This differential is indicative of substantial slip between the two phases, where the gas phase moves more freely relative to the liquid, enhancing its velocity relative to that predicted by homogeneous models. These observations align with findings from Kawahara *et al.*, [26], who noted that traditional homogeneous models often fail to accurately predict the void fraction in regimes where significant phase slip occurs, particularly in annular and churn flows. Their research emphasizes the need for more nuanced models that account for the complex dynamics of two-phase flow, especially in microchannel environments where the effects of phase slip and interfacial tension dramatically influence flow behavior.

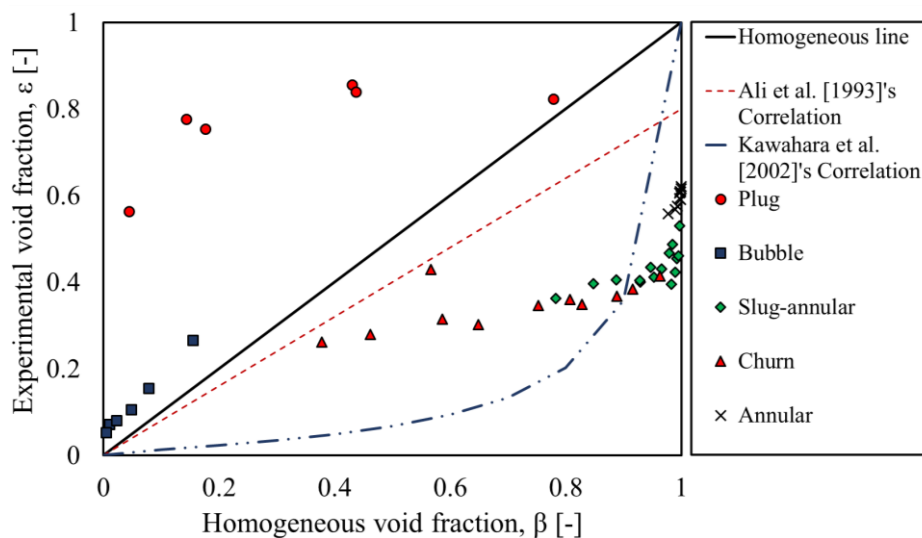


**Fig. 15.** Comparison of homogeneous and measured void fraction

Pressure gradient, defined as the pressure drop per unit length, provides critical insights into the behavior of two-phase flows in microchannels. Figure 16 presents experimental data illustrating how the pressure gradient varies as a function of the  $J_G$  and  $J_L$ . It is evident from the data that the pressure gradient increases with increases in both  $J_G$  and  $J_L$ , underscoring the significant impact these velocities have on the flow dynamics within the channel.

This relationship is consistent with findings from Awad and Muzychka [40], who explored two-phase flow modeling in microchannels and minichannels, emphasizing how superficial velocities influence the frictional pressure gradients. Their research provides valuable context, indicating that both the gas and liquid velocities play crucial roles in enhancing the frictional forces within the flow, leading to higher pressure gradients. Furthermore, the interplay between  $J_G$  and  $J_L$  in determining the pressure gradient aligns with the dynamics of two-phase flow regimes as discussed by Sur and Liu [14], who noted that varying these velocities could significantly shift flow patterns and consequently affect pressure gradients. Their study highlights the importance of accurately modeling these parameters to predict and manage the behavior of two-phase systems effectively.

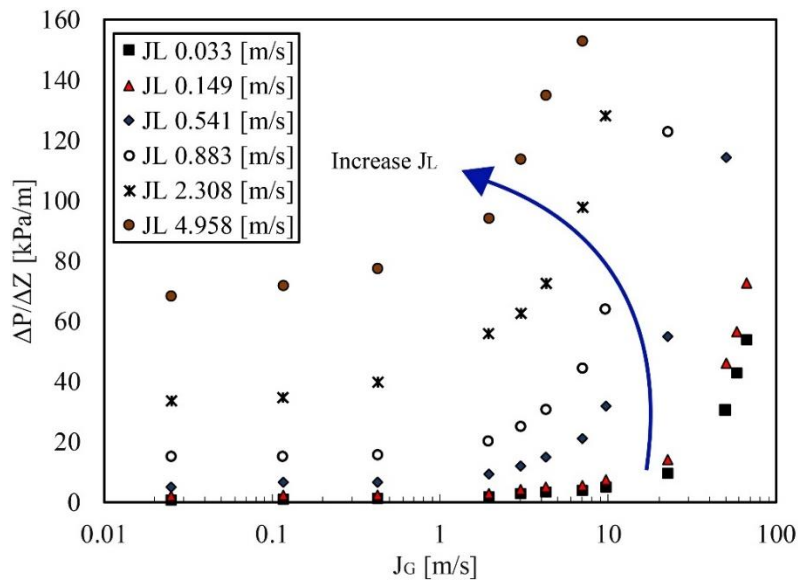


Fig. 16. Pressure gradient as a function of  $J_L$  and  $J_G$

#### 4. Conclusions

The conclusions of the study are as follows

- i. This study successfully identified several important flow patterns, including plug, slug-annular, annular, disperse bubble, and churn flows, each displaying unique characteristics influenced by operational conditions and the physical properties of the fluids.
- ii. The superficial velocities of both gas and liquid were found to significantly impact the formed flow patterns, void fraction, and pressure gradient.
- iii. Void fraction was getting higher as the  $J_G$  increased.
- iv. Increases in both gas and liquid superficial velocities tend to enhance the complexity of the interactions between the gas and liquid, leading to significant changes in flow patterns and pressure gradients. Pressure gradients specifically, was increased.
- v. The transition line between slug-annular and annular flows towards churn flow shifts towards higher liquid superficial velocities ( $J_L$ ). This phenomenon is associated with increased liquid viscosity and decreased surface tension, which slow down the movement of the liquid and facilitate the formation of the gas phase, affecting the stability and phase distribution within the flow.

#### References

- [1] López-Belchí, Alejandro, Fernando Illan-Gomez, Francisco Vera-García, and Jose R. García-Cascales. "Experimental condensing two-phase frictional pressure drop inside mini-channels. Comparisons and new model development." *International Journal of Heat and Mass Transfer* 75 (2014): 581-591. <https://doi.org/10.1016/j.ijheatmasstransfer.2014.04.003>
- [2] Ramirez-Rivera, Francisco, Alejandro Lopez-Belchi, Francisco Vera-Garcia, J. R. García-Cascales, and Fernando Illan-Gomez. "Two phase flow pressure drop in multiport mini-channel tubes using R134a and R32 as working fluids." *International Journal of Thermal Sciences* 92 (2015): 17-33. <https://doi.org/10.1016/j.ijthermalsci.2015.01.014>
- [3] Li, Sheng, Chaojun Fan, Jun Han, Mingkun Luo, Zhenhua Yang, and Huijie Bi. "A fully coupled thermal-hydraulic-mechanical model with two-phase flow for coalbed methane extraction." *Journal of Natural Gas Science and Engineering* 33 (2016): 324-336. <https://doi.org/10.1016/j.jngse.2016.05.032>
- [4] Kim, Sung-Min, and Issam Mudawar. "Theoretical model for local heat transfer coefficient for annular flow boiling in circular mini/micro-channels." *International Journal of Heat and Mass Transfer* 73 (2014): 731-742. <https://doi.org/10.1016/j.ijheatmasstransfer.2014.02.055>
- [5] Mahvi, Allison J., and Srinivas Garimella. "Modeling framework to predict two-phase flow distribution in heat

- exchanger headers." *International Journal of Refrigeration* 104 (2019): 65-75. <https://doi.org/10.1016/j.ijrefrig.2019.04.031>
- [6] Pellicone, Devin, Alfonso Ortega, Marcelo del Valle, and Steven Schon. "Simulation of Two-Phase Flow and Heat Transfer for Practical Design of Mini-and Micro-Channel Heat Exchangers." In *ASME International Mechanical Engineering Congress and Exposition*, vol. 54921, pp. 517-525. 2011. <https://doi.org/10.1115/IMECE2011-63637>
- [7] Triplett, K. A., S. M. Ghiaasiaan, S. I. Abdel-Khalik, A. LeMouel, and B. N. McCord. "Gas-liquid two-phase flow in microchannels: part II: void fraction and pressure drop." *International Journal of Multiphase Flow* 25, no. 3 (1999): 395-410. [https://doi.org/10.1016/S0301-9322\(98\)00055-X](https://doi.org/10.1016/S0301-9322(98)00055-X)
- [8] Serizawa, Akimi, Ziping Feng, and Zensaku Kawara. "Two-phase flow in microchannels." *Experimental Thermal and Fluid Science* 26, no. 6-7 (2002): 703-714. [https://doi.org/10.1016/S0894-1777\(02\)00175-9](https://doi.org/10.1016/S0894-1777(02)00175-9)
- [9] Kawaji, M., and P. M.-Y. Chung. "Adiabatic gas-liquid flow in microchannels." *Microscale Thermophysical Engineering* 8, no. 3 (2004): 239-257. <https://doi.org/10.1080/10893950490477518>
- [10] Pehlivan, K., I. Hassan, and M. Vaillancourt. "Experimental study on two-phase flow and pressure drop in millimeter-size channels." *Applied Thermal Engineering* 26, no. 14-15 (2006): 1506-1514. <https://doi.org/10.1016/j.applthermaleng.2005.12.010>
- [11] Lee, Chi Young, and Sang Yong Lee. "Influence of surface wettability on transition of two-phase flow pattern in round mini-channels." *International Journal of Multiphase Flow* 34, no. 7 (2008): 706-711. <https://doi.org/10.1016/j.ijmultiphaseflow.2008.01.002>
- [12] Saisorn, Sira, and Somchai Wongwises. "Flow pattern, void fraction and pressure drop of two-phase air-water flow in a horizontal circular micro-channel." *Experimental Thermal and Fluid Science* 32, no. 3 (2008): 748-760. <https://doi.org/10.1016/j.expthermflusci.2007.09.005>
- [13] Hanafizadeh, P., M. H. Saidi, A. Nouri Gheimasi, and S. Ghanbarzadeh. "Experimental investigation of air-water, two-phase flow regimes in vertical mini pipe." *Scientia Iranica. Transaction B, Mechanical Engineering* 18, no. 4 (2011): 923. <https://doi.org/10.1016/j.scient.2011.07.003>
- [14] Sur, Aritra, and Dong Liu. "Adiabatic air-water two-phase flow in circular microchannels." *International Journal of Thermal Sciences* 53 (2012): 18-34. <https://doi.org/10.1016/j.ijthermalsci.2011.09.021>
- [15] Li, Shidong, Luky Hendraningrat, and Ole Torsaeter. "Improved oil recovery by hydrophilic silica nanoparticles suspension: 2 phase flow experimental studies." In *IPTC 2013: International Petroleum Technology Conference*, pp. cp-350. European Association of Geoscientists & Engineers, 2013. <https://doi.org/10.2523/16707-MS>
- [16] Li, Hong-Wei, Yun-Long Zhou, Yan-Dong Hou, Bin Sun, and Yue Yang. "Flow pattern map and time-frequency spectrum characteristics of nitrogen-water two-phase flow in small vertical upward noncircular channels." *Experimental Thermal and Fluid Science* 54 (2014): 47-60. <https://doi.org/10.1016/j.expthermflusci.2014.01.017>
- [17] Pipathattakul, Manop, Omid Mahian, Ahmet Selim Dalkilic, and Somchai Wongwises. "Effects of the gap size on the flow pattern maps in a mini-gap annular channel." *Experimental Thermal and Fluid Science* 57 (2014): 420-424. <https://doi.org/10.1016/j.expthermflusci.2014.06.006>
- [18] Lu, Qi, Deqi Chen, and Qinghua Wang. "Visual investigation on the interface morphology of Taylor bubble and the characteristics of two-phase flow in mini-channel." *Chemical Engineering Science* 134 (2015): 96-107. <https://doi.org/10.1016/j.ces.2015.04.042>
- [19] Kim, Seok, and Sang Yong Lee. "Split of two-phase plug flow with elongated bubbles at a microscale branching T-junction." *Chemical Engineering Science* 134 (2015): 119-128. <https://doi.org/10.1016/j.ces.2015.04.020>
- [20] Sudarja, Sudarja, Sukamta Sukamta, and Fauzan Saputra. "Investigation of flow pattern and void fraction of air and low surface tension liquid in A 30° inclined small pipe." *Journal of Advanced Research in Fluid Mechanics and Thermal Sciences* 83, no. 2 (2021): 73-83. <https://doi.org/10.37934/arfmts.83.2.7383>
- [21] Shin, Hong-Cheol, and Sung-Min Kim. "Experimental investigation of two-phase flow regimes in rectangular micro-channel with two mixer types." *Chemical Engineering Journal* 448 (2022): 137581. <https://doi.org/10.1016/j.cej.2022.137581>
- [22] Fang, Yidong, Di Lu, Wenliang Yang, Huinan Yang, and Yuqi Huang. "Saturated flow boiling heat transfer of R1233zd (E) in parallel mini-channels: Experimental study and flow-pattern-based prediction." *International Journal of Heat and Mass Transfer* 216 (2023): 124608. <https://doi.org/10.1016/j.ijheatmasstransfer.2023.124608>
- [23] Mahdi, Louay Abd Al-Azez, Hasanain Adnan Abdul Wahhab, and Miqdam Tariq Chaichan. "The Change of Flow Pattern from Stratified to Stratified-Wavy for Condensation in Wire on Tube Heat Exchangers." *Journal of Advanced Research in Fluid Mechanics and Thermal Sciences* 117, no. 2 (2024): 105-115. <https://doi.org/10.37934/arfmts.117.2.105115>
- [24] Ejim, C. E., M. A. Rahman, A. Amirfazli, and B. A. Fleck. "Effects of liquid viscosity and surface tension on atomization in two-phase, gas/liquid fluid coker nozzles." *Fuel* 89, no. 8 (2010): 1872-1882. <https://doi.org/10.1016/j.fuel.2010.03.005>
- [25] Erfani, Amir, Shahin Khosharay, and Clint P. Aichele. "Surface tension and interfacial compositions of binary

- glycerol/alcohol mixtures." *The Journal of Chemical Thermodynamics* 135 (2019): 241-251. <https://doi.org/10.1016/j.jct.2019.03.014>
- [26] Kawahara, A., P. M.-Y. Chung, and M. Kawaji. "Investigation of two-phase flow pattern, void fraction and pressure drop in a microchannel." *International Journal of Multiphase Flow* 28, no. 9 (2002): 1411-1435. [https://doi.org/10.1016/S0301-9322\(02\)00037-X](https://doi.org/10.1016/S0301-9322(02)00037-X)
- [27] Chung, P. M.-Y., and M. Kawaji. "The effect of channel diameter on adiabatic two-phase flow characteristics in microchannels." *International Journal of Multiphase Flow* 30, no. 7-8 (2004): 735-761. <https://doi.org/10.1016/j.ijmultiphaseflow.2004.05.002>
- [28] Kovalev, Alexander, Anna Yagodnitsyna, and Artur Bilsky. "Plug flow of immiscible liquids with low viscosity ratio in serpentine microchannels." *Chemical Engineering Journal* 417 (2021): 127933. <https://doi.org/10.1016/j.cej.2020.127933>
- [29] Tice, Joshua D., Adam D. Lyon, and Rustem F. Ismagilov. "Effects of viscosity on droplet formation and mixing in microfluidic channels." *Analytica Chimica Acta* 507, no. 1 (2004): 73-77. <https://doi.org/10.1016/j.aca.2003.11.024>
- [30] Kim, Jonghyun, and Joon Sang Lee. "Effects of surface tension and inclined surface wettability on sliding bubble heat transfer." *International Journal of Thermal Sciences* 142 (2019): 77-88. <https://doi.org/10.1016/j.ijthermalsci.2019.04.013>
- [31] Sudarja, Sudarja, and Sukamta Sukamta. "Experimental Study on Flow Pattern and Void Fraction of Air-Water and 3% Butanol Two-Phase Flow in 30° Inclined Mini Channel." *Journal of Advanced Research in Experimental Fluid Mechanics and Heat Transfer* 1, no. 1 (2020): 11-20.
- [32] Chen, Shulei, Kun Liu, Cunbin Liu, Dongyang Wang, Dechun Ba, Yuanhua Xie, Guangyu Du, Yaoshuai Ba, and Qiao Lin. "Effects of surface tension and viscosity on the forming and transferring process of microscale droplets." *Applied Surface Science* 388 (2016): 196-202. <https://doi.org/10.1016/j.apsusc.2016.01.205>
- [33] Boogar, Rahman Sadeghi, Reza Gheshlaghi, and Mahmood Akhavan Mahdavi. "The effects of viscosity, surface tension, and flow rate on gasoil-water flow pattern in microchannels." *Korean Journal of Chemical Engineering* 30 (2013): 45-49. <https://doi.org/10.1007/s11814-012-0119-8>
- [34] Guo, Zhenyi, David F. Fletcher, and Brian S. Haynes. "Numerical simulation of annular flow hydrodynamics in microchannels." *Computers & Fluids* 133 (2016): 90-102. <https://doi.org/10.1016/j.compfluid.2016.04.017>
- [35] Sudarja, Aqli Haq, Deendarlianto, Indarto, and Adhika Widyaparaga. "Experimental study on the flow pattern and pressure gradient of air-water two-phase flow in a horizontal circular mini-channel." *Journal of Hydrodynamics* 31 (2019): 102-116. <https://doi.org/10.1007/s42241-018-0126-2>
- [36] Yue, Jun, Lingai Luo, Yves Gonthier, Guangwen Chen, and Quan Yuan. "An experimental investigation of gas-liquid two-phase flow in single microchannel contactors." *Chemical Engineering Science* 63, no. 16 (2008): 4189-4202. <https://doi.org/10.1016/j.ces.2008.05.032>
- [37] Vozhakov, Ivan S., and Fedor V. Ronshin. "Experimental and theoretical study of two-phase flow in wide microchannels." *International Journal of Heat and Mass Transfer* 136 (2019): 312-323. <https://doi.org/10.1016/j.ijheatmasstransfer.2019.02.099>
- [38] Triplett, Ka A., S. M. Ghiaasiaan, S. I. Abdel-Khalik, and D. L. Sadowski. "Gas-liquid two-phase flow in microchannels Part I: two-phase flow patterns." *International Journal of Multiphase Flow* 25, no. 3 (1999): 377-394. [https://doi.org/10.1016/S0301-9322\(98\)00054-8](https://doi.org/10.1016/S0301-9322(98)00054-8)
- [39] Zhang, Tong, Bin Cao, Yilin Fan, Yves Gonthier, Lingai Luo, and Shudong Wang. "Gas-liquid flow in circular microchannel. Part I: Influence of liquid physical properties and channel diameter on flow patterns." *Chemical Engineering Science* 66, no. 23 (2011): 5791-5803. <https://doi.org/10.1016/j.ces.2011.07.035>
- [40] Awad, M. M., and Y. S. Muzychka. "Two-phase flow modeling in microchannels and minichannels." *Heat Transfer Engineering* 31, no. 13 (2010): 1023-1033. <https://doi.org/10.1080/01457631003639059>